Journal of Porphyrins and Phthalocyanines
J. Porphyrins Phthalocyanines 2010; **14**: 646–659
DOI: 10.1142/S1088424610002483

Published at http://www.worldscinet.com/jpp/

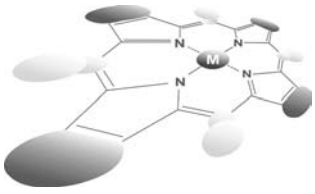

Chiral "basket handle" binaphthyl porphyrins: synthesis, catalytic epoxidation and NMR conformational studies

Eric Rose*[a◊], Emma Gallo[b◊], Nicolas Raoul[a], Léa Bouché[a], Ariane Pille[a], Alessandro Caselli[b] and Olivier Lequin*[c]

[a] *Université Pierre et Marie Curie, UPMC Univ Paris 06, IPCM, UMR CNRS 7201, Laboratoire de Synthèse Organique et Organométallique, Case 181, 4 place Jussieu, F-75252 Paris Cedex 05, France*
[b] *Dipartimento di Chimica Inorganica, Metallorganica e Analitica "Lamberto Malatesta", Università di Milano, and ISTM-CNR, Via Venezian 21, 20133 Milano, Italy*
[c] *Université Pierre et Marie Curie, UPMC Univ Paris 06, Laboratoire des Biomolécules, UMR CNRS 7203, Case 182, 4 place Jussieu, F-75252 Paris Cedex 05, France*

Received 21 May 2010
Accepted 29 June 2010

ABSTRACT: Three "basket handle" porphyrins have been prepared by condensation of tetrakis-(α,β,α,β-2-aminophenyl)porphyrin atropoisomer with 1,1′-binaphthyl, 2,2′-dimethoxy, -3,3′-dicarbonylchloride, -3,3′-diacetylchloride and -3,3′-dipropanoylchloride. The epoxidation of styrene with the three iron catalysts, obtained after metalation of the free porphyrins, occurs with good yields and moderate *ee* up to 54%. These porphyrins showed unexpected conformational differences, as revealed by NMR spectroscopy. In particular, variable temperature NMR studies showed that the methoxy group in one of them undergoes intermediate conformational exchange on the ^{1}H NMR time scale at room temperature. Lowering the temperature to -50 °C revealed the presence of four states in slow exchange on the NMR time scale. These results evidence a dynamic conformational equilibrium of the binaphthyl handles that adopt different, asymmetric positions with respect to the porphyrin plane.

KEYWORDS: chiral porphyrin, NMR, conformational exchange, binaphthyl porphyrin, enantioselective epoxidation.

INTRODUCTION

Previous studies have shown that synthetic porphyrins can be excellent structural and functional analogs of the active sites of hemoproteins. For instance, efficient models of myoglobin Mb [1] and cytochrome c oxidase CcO [2] have been described. For enantioselective reactions such as epoxidation [3], cyclopropanation [4], aziridination [5], amination [6] and functionalization of non-activated C-H bonds [7], prodigious effort has been devoted to obtain catalysts using the rigid core of a porphyrin and judicious functionalization of the periphery of the macrocycle [8]. In this context, binaphthyl porphyrins have appeared to be interesting chiral porphyrins [9] since the pioneering work of Groves *et al.* in 1983 [10], who first reported the synthesis of **1** (Fig. 1), a compound still of interest. Collman, Rose *et al.* later developed the synthesis of a chiral porphyrin $\alpha\alpha\beta\beta\mathbf{C_1}$ for the enantioselective epoxidation of olefins by condensation of the tetrakis-ααββ-(2-aminophenyl)porphyrin atropoisomer $TAPPH_2$ with (*R*)-2,2′-dimethoxy,-3,3′-dichlorocarbonyl-1,1′-binaphthyl $\mathbf{BN_1}$ (Fig. 2) [11]. After metalation with $FeCl_2$, $\mathbf{Fe\alpha\alpha\beta\beta C_1}$ used for the epoxidation of styrene, as an example [11], gave the (*S*) styrene epoxide in 95% yield and 83% ee and turnover up to 5500 while maintaining a reasonable ee of 75% at a rate of 40 turnovers/min. An oxidative modification of the catalyst is observed at the beginning of the reaction *via* a suggested oxidative demethylation to form a quinone type catalyst **2** (Fig. 3).

◊SPP full member in good standing

*Correspondence to: Eric Rose, eric.rose@upmc.fr and Olivier Lequin, olivier.lequin@upmc.fr

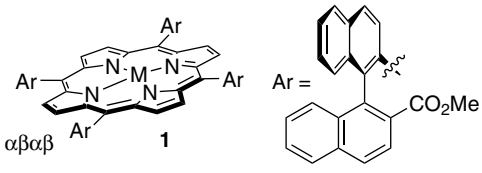

Fig. 1. Groves binaphthyl porphyrin

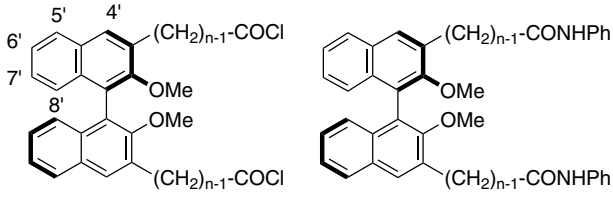

Fig. 2. Binaphthyl derivatives

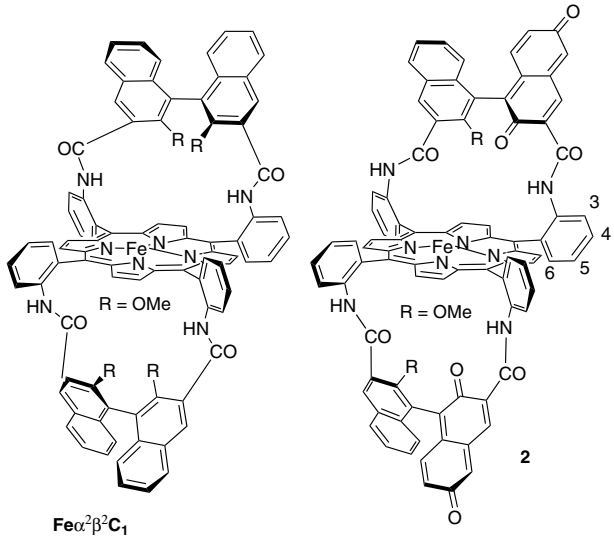

Fig. 3. FeαβαβC_1 porphyrin and modified catalyst

Rose *et al.* obtained a new **FeαααββC_2** catalyst by homologation of the binaphthyl handle **BN_1** into a new 1,1′-binaphthyl, 2,2′-dimethoxy, 3,3′-dicarbonylchloride **BN_2** which gave the epoxide with the opposite configuration, the (*R*) styrene epoxide with ee > 97% and turnover up to 1500 [12]. In this case, the methoxy group remains untouched as it is too far from the [Fe=O] active site. Du, Woo and Rose used the iron catalyst **FeαααββC_1** to perform cyclopropanation of olefins with diazoacetate [13]. Since Zhang, Gallo *et al.* [14] independently had shown that Co porphyrin complexes could also undertake cyclopropanation [15], Gallo, Rose *et al.* extended this study to perform enantioselective cyclopropanation of olefins catalyzed by Co-porphyrins using **CoααββC_2** and another catalyst **CoααββC_3** obtained after condensation of the bis-homologated binaphthyl handle (Fig. 4) [16]. The porphyrin with the shortest handle **CoααββC_1** was devoid of catalytic activity. The enantioselectivities observed, up to 90% ee with *cis*/*trans* ratio reaching 11:89, were not as high as those obtained for epoxidation

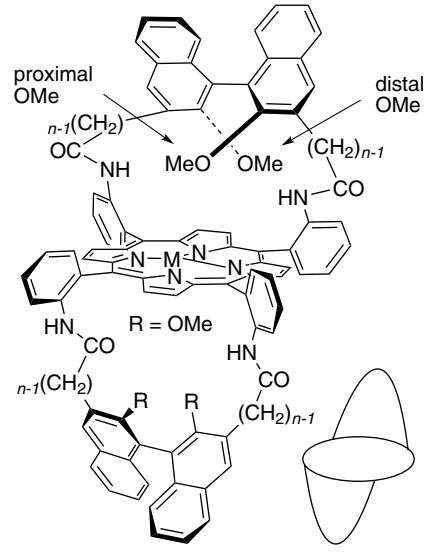

Fig. 4. Metallo **αααββC_n** porphyrins

but of course the intermediates which involve a metal oxo and a metallocarbene double bond cannot be compared.

We describe herein the preparation of three porphyrins **αβαβC_n** obtained by condensation of binaphthyl handles **BN_n** (n = 1–3) with the αβαβ atropoisomer of tetrakis-(2-aminophenyl)porphyrin **$TAPPH_2$**, their ^{1}H and ^{13}C NMR studies and epoxidation of styrene with the corresponding Fe-catalysts to shed light on the influence of the handle attachment to the 5,10- and 15,20-positions of the *meso*-2-aminophenyl groups compared to the 5,15- and 10,20-*meso*-positions in enantioselective catalysis.

RESULTS

Synthesis

Tetrakis-(2-aminophenyl)porphyrins ***o*-$TAPPH_2$** were prepared by reduction of the corresponding tetrakis-(2-nitrophenyl)porphyrins ***o*-$TNPPH_2$**, which were obtained by condensation of pyrrole with 2-nitrobenzaldehyde [1]. The statistical mixture of the four atropoisomers **αβαβ**, **αααββ**, **αααβ** and **αααα-*o*-$TAPPH_2$** was separated by silica gel chromatography column in the ratio 12.5, 25, 50 and 12.5%. The abundance of the four atropoisomers can be changed by thermal treatment of the corresponding nitrophenyl atropoisomers or their Zn derivatives to yield as the major atropoisomer the **αβαβ** [20] or the **αααββ** one, respectively [21]. We also prepared the binaphthyl diacid chlorides **BN_n** [12, 22], n represents the number of carbons between the binaphthyl residue starting from the (R)-(+)-1,1′-Bi-2-naphthol. Thus, condensation of the **αβαβ** aminoporphyrin with the acid chlorides using high dilution technique with a syringe pump [11, 12] afforded the free-base symmetrical porphyrins **αβαβC_n** (n = 1–3), respectively in 87, 38 and 26% yield (Chart 1). The goal

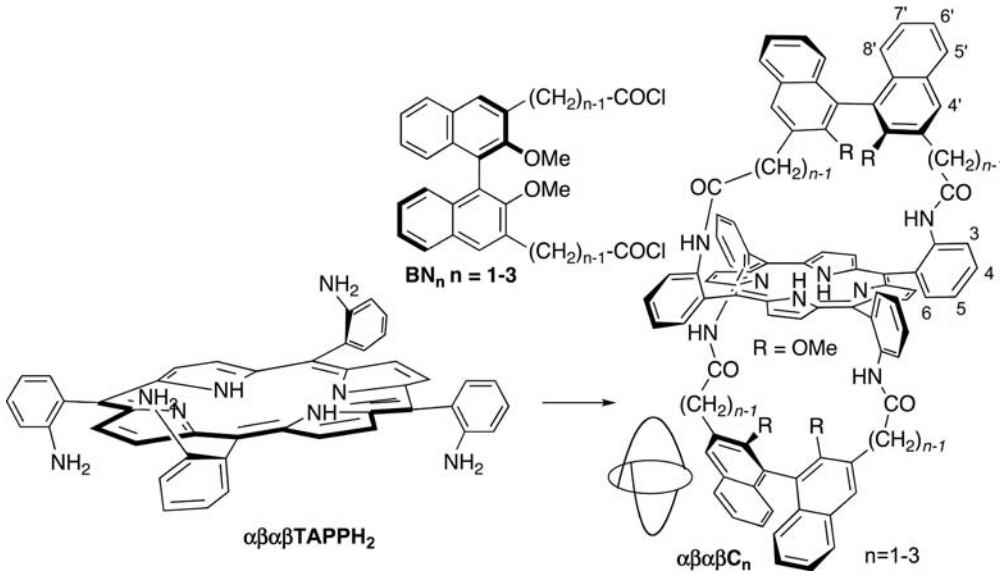

Chart 1. Preparation of **αβαβC$_n$** porphyrins

was to compare the influence of the handle attachment to the *meso*-2-aminophenyl groups (at 5,10 and 15,20-positions compared to 5,15 and 10,20-*meso*-positions) in enantioselective catalysis.

NMR assignments

In the absence of X-ray structures of our porphyrins, we undertook their studies by NMR spectroscopy. The ^{1}H NMR spectra of the three porphyrins are shown in Fig. 5. The spectra exhibit limited sets of resonances (comprising 15 to 17 unequivalent resonances for 70 to 86 protons), indicating high symmetry for these porphyrins **αβαβC$_n$**. We will discuss successively the chemical shift values of the NH pyrrolic and amidophenyl protons, of the *meso*-phenyl groups, of the β-pyrrolic and the binaphthyl handle protons, and finally of the protons of the methoxy groups which are the best observers of the porphyrin plane.

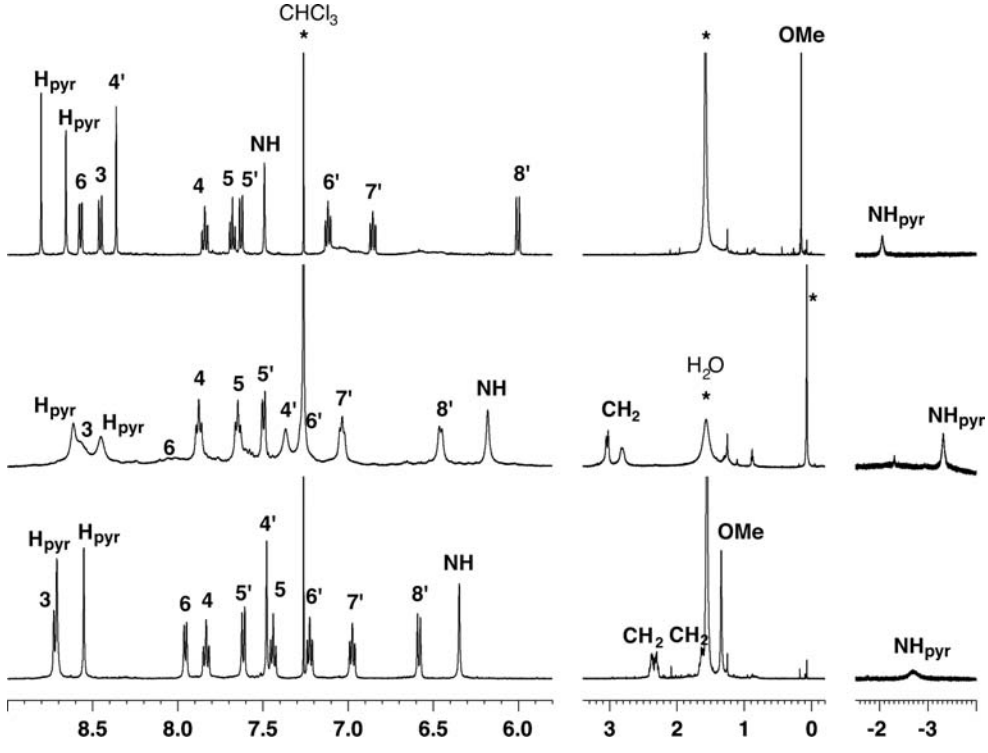

Fig. 5. ^{1}H NMR spectra of **αβαβC$_n$** porphyrins (500 MHz, $CDCl_3$, 20 °C). Top, **αβαβC$_1$**; middle, **αβαβC$_2$**; bottom, **αβαβC$_3$**. Solvent signal or impurities are indicated by an asterisk. The scale of the NH pyrrolic region has been multiplied by four

Pyrrolic NH protons. The chemical shifts of these protons are sensitive to the deformation of the porphyrin plane. The more planar the macrocycle, the more upfield-shifted are their chemical shifts [23]. The signals of the pyrrolic NH of the three porphyrins **αβαβC$_1$**, **αβαβC$_2$** and **αβαβC$_3$** resonate at -2.06, -3.31 and -2.70 ppm in $CDCl_3$. This indicates that in **αβαβC$_1$**with the shortest handle, the porphyrin plane has to be distorted to accommodate the two binaphthyl residues, the porphyrin ring causing a smaller shielding anisotropy on the NH protons. For the other two porphyrins, the NH protons resonate at expected chemical shift values for planar or slightly deformed macrocycles.

Amidophenyl amide protons. The amidophenyl amide protons of **αβαβC$_1$**, **αβαβC$_2$** and **αβαβC$_3$** resonate at 7.49, 6.18 and 6.35 ppm, respectively, in $CDCl_3$. The most deshielded protons belong to the non-homologated porphyrin **αβαβC$_1$** which is again in good agreement with a non-planar macrocycle and a smaller anisotropy effect of the porphyrin ring.

Meso-phenyl protons. The nearest hydrogen of the *meso*-phenyl group, namely the H_6 proton, occupies a key spectator position of the binaphthyl handle. Therefore, it is important to assign unambiguously its chemical shift. Indeed the four aromatic protons H_3-H_6 resonate as two apparent doublets H_3 and H_6 (J ~ 8 Hz) and two apparent triplets H_4 and H_5 (J ~ 8 Hz). The *meso*-phenyl protons of other tetrakis-(2-amidophenyl)porphyrins have been tentatively assigned previously [24]. However Perlmutter *et al.* [25] and our group [26] proved definitively by two different NMR techniques that this is the H_6 proton and not the H_3 proton which is the more shielded *meso*-aryl proton. Perlmutter *et al.* used an elegant application of ^{1}H NMR Nuclear-Overhauser technique and we did selective ^{1}H-^{13}C decoupling of the H_3 proton, which transformed the ^{13}C off-resonance doublet of the corresponding carbon C_3 to a singlet. The phenyl protons of **αβαβC$_1$**, **αβαβC$_2$** and **αβαβC$_3$** porphyrins in this work were unambiguously assigned from the analysis of 2D ^{1}H-^{13}C HMBC experiments (Table 1). In particular, carbon C_3 could be assigned through a correlation with NH proton. The assignment of other aromatic resonances was based on the observation of typical $^3J_{H,C}$ correlations in phenyl groups. For these porphyrins, the H_4 protons resonate at approximately the same frequency at 7.84, 7.88 and 7.83 ppm.

Table 1. ^{1}H chemical shifts of the *meso*-phenyl groups of **αβαβC$_n$** and **ααββC$_n$** porphyrins

Entry	Compound[a]	ArH_3	ArH_4	ArH_5	ArH_6
1	αβαβC$_1$	8.45	7.84	7.68	8.57
2	αβαβC$_2$	8.57	7.88	7.65	8.00
3	αβαβC$_3$	8.72	7.83	7.44	7.95
4	ααββC$_1$	8.40	7.92	7.82	9.11
		8.33	7.90	7.69	8.86
5	ααββC$_2$	8.85	7.89	7.57	8.15
		8.54	7.82	7.47	7.62
6	ααββC$_3$	8.70	7.92	7.52	7.90
		8.20	7.78	7.78	7.52

[a] $CDCl_3$, 20 °C, 500 MHz.

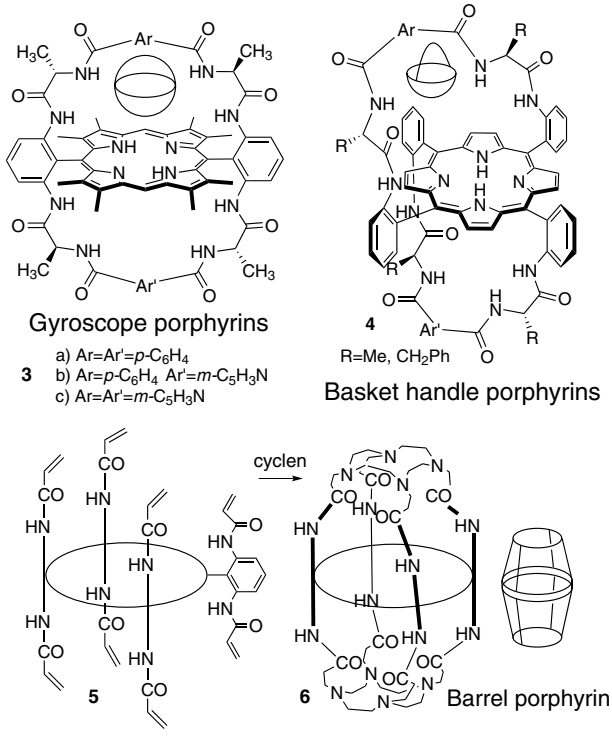

Fig. 6. Amidophenylporphyrins

This is a fingerprint of these 2-amidophenyl porphyrins because similar chemical shift values have been observed in all the porphyrins that we prepared previously: the "gyroscope" porphyrin **3** [27], the "basket handle" porphyrins **4** [28], the "barrel" porphyrin **6** obtained by Michael addition of cyclen to the octa-acceptor **5** [29] and the **αααββC$_{1\text{-}3}$** binaphthyl porphyrins [12] (Fig. 6).

Proton H_6 experiences a very different chemical shift in **αβαβC$_1$** in comparison with its **C$_2$** and **C$_3$** counterparts, being the most unshielded proton. Indeed, the H_6 signal is observed at 8.57, 8.00 and 7.95 ppm, the shielding of this proton increasing with the length of the handle. Thus the deshielded H_6 protons in **αβαβC$_1$** porphyrin are less influenced by the anisotropy cone of the macrocycle, in good agreement again with a deformation of the porphyrin plane. Interestingly, the H_3 and H_6 protons exhibit larger linewidths in **αβαβC$_2$** porphyrin, as compared to the other two, proton H_6 being hardly observable. This observation will be discussed in relation with methoxy protons broadening, *vide infra*.

β-pyrrolic protons. The β-pyrrolic protons resonate as two sets of two singlets integrating for four protons each, as is expected in the case of fast-exchange NH tautomerism and for symmetry reasons [24a] yielding two groups (2,3,12,13 and 7,8,17,18) of magnetically equivalent protons. Thus, peaks at 8.80 and 8.66 ppm are found for the

Table 2. ^{1}H chemical shifts of the naphthyl groups of **αβαβC$_n$** porphyrins

Compounds[a]	$H_{4'}$(s)	$H_{5'}$(d)	$H_{6'}$(t)	$H_{7'}$(t)	$H_{8'}$(d)	OMe	NH amide	NH pyrrole
αβαβC$_1$	8.36	7.63	7.12	6.85	6.00	0.15	7.49	-2.06
BINAP$_1$	9.01	7.16	7.42	7.53	8.11	3.46	9.98	—
Δδ[b]	0.65	-0.47	0.30	0.68	2.11	3.31	2.49	—
αβαβC$_2$	7.37	7.50	7.28	7.03	6.46	~0[c]	6.18	-3.31
BINAP$_2$	8.02	7.24	7.02	7.43	7.89	3.27	8.07	—
Δδ[b]	0.65	-0.26	-0.26	0.40	1.43	~-3.3	1.89	—
αβαβC$_3$	7.48	7.61	7.22	6.97	6.58	1.34	6.35	-2.70
BINAP$_3$	7.85	7.12	7.17	7.36	7.80	3.19	8.42	—
Δδ[b]	0.37	-0.49	-0.05	0.39	1.22	1.85	2.07	—

[a] $CDCl_3$, 20 °C, 500 MHz. [b] Δδ = δ(BINAP$_n$) - δ(ααββC$_n$ porphyrin). [c] Very broad.

αβαβC$_1$ porphyrin whereas peaks at 8.61 and 8.45 are observed for the **αβαβC$_2$** porphyrin and peaks at 8.71 and 8.55 for the **αβαβC$_3$** porphyrin.

Naphthalenic protons. The synthesis of binaphthyl handles substituted by CONHPh, CH_2CONHPh and $(CH_2)_2$CONHPh **BINAP$_{1\text{-}3}$** (Fig. 2) has been undertaken to obtain model compounds, *vide supra*, and to know which proton is the most shielded by the anisotropy of the porphyrin during the condensation of the handle to the tetraaminoporphyrin. The chemical shifts are reported in Table 2. The ten protons of the naphthyl residue resonate as five peaks with one singulet for the protons $H_{4'}$, two doublets for the protons $H_{5'}$ and $H_{8'}$ and two triplets for the protons $H_{6'}$ and $H_{7'}$ [30].

Methoxy protons. The methoxy groups of the **αβαβC$_1$** and **αβαβC$_3$** porphyrins resonate respectively at 0.15 and 1.34 ppm as a sharp signal in $CDCl_3$. The methoxy groups are shielded by 3.31 and 1.85 ppm with respect to the amido models **BINAP$_{1\text{-}3}$** (Fig. 2, Table 3). Unexpectedly, for the basket handle **αβαβC$_2$** porphyrin, we did not observe a sharp signal for the 12 protons of the four methoxy groups. By analyzing more deeply the ^{1}H NMR spectrum, an unexpected very broad, flat peak was found between 0.5 and -1.5 pm.

Table 3. ^{1}H chemical shifts of the OMe groups of **αβαβC$_n$** and **ααββC$_n$** porphyrins

Entry	Compound[a]	δ(OMe) distal[a]	δ(OMe) proximal[a]
1	αβαβC$_1$	2.97	-0.63
2	BINAP$_1$	3.46	—
3	Δδ[b]	0.49	4.09
4	αβαβC$_2$	1.98	-0.51
5	BINAP$_2$	3.27	—
6	Δδ[b]	1.29	3.78
7	αβαβC$_3$	2.34	1.86
8	BINAP$_3$	3.19	—
9	Δδ[b]	0.85	1.33
10	αβαβC$_1$	0.15	—
11	Δδ	3.31	—
12	αβαβC$_2$	~0[c]	—
13	Δδ	~-3.3 ppm	—
14	αβαβC$_3$	1.34	—
15	Δδ	1.85	—

[a] $CDCl_3$, 20 °C, 500 MHz. [b] Δδ = δ(BINAP$_n$) - δ(ααββC$_n$ porphyrin). [c] Very broad.

^{1}H, ^{13}C NMR data at different temperatures

A possible explanation of the broadening at room temperature of the methoxy proton signal in **αβαβC$_2$** porphyrin is a conformational equilibrium in intermediate exchange on the ^{1}H NMR time scale. In order to probe the dynamics and the nature of this conformational transition, we decided to perform variable temperature ^{1}H NMR studies on **αβαβC$_2$**, as well as on **αβαβC$_1$** and **αβαβC$_3$** porphyrins. A gradually increasing of the temperature to 40 °C induces an increase of the peak height of the methoxy group in $CDCl_3$, as well as that of H_3 and H_6 protons (Fig. 7), in good agreement with a faster exchange on the ^{1}H NMR time scale. Conversely, a gradual lowering of the temperature to -30 °C in $CDCl_3$ induces a severe broadening of most resonances. In contrast, the spectra recorded at the lowest temperatures (-40 °C and -50 °C) are characterized by sharp lines and show a high complexity due to numerous splittings of aromatic and aliphatic resonances, indicating a slow exchange regime on the ^{1}H NMR time scale for all resonances. These spectral changes are fully reversible upon warming up to room temperature. In order to characterize the different magnetic environments observed at low temperature, 2D NMR spectra were recorded at -50 °C. The 2D ^{1}H-^{13}C HSQC spectrum (Fig. 8) reveals that up to four environments can be observed for each aromatic and aliphatic CH resonance. Four distinct correlation pathways could be assigned for the aromatic spin systems in the 2D ^{1}H-^{1}H COSY experiments. The four sets of chemical shifts can be divided into two different subgroups of almost equivalent signals (or closed to

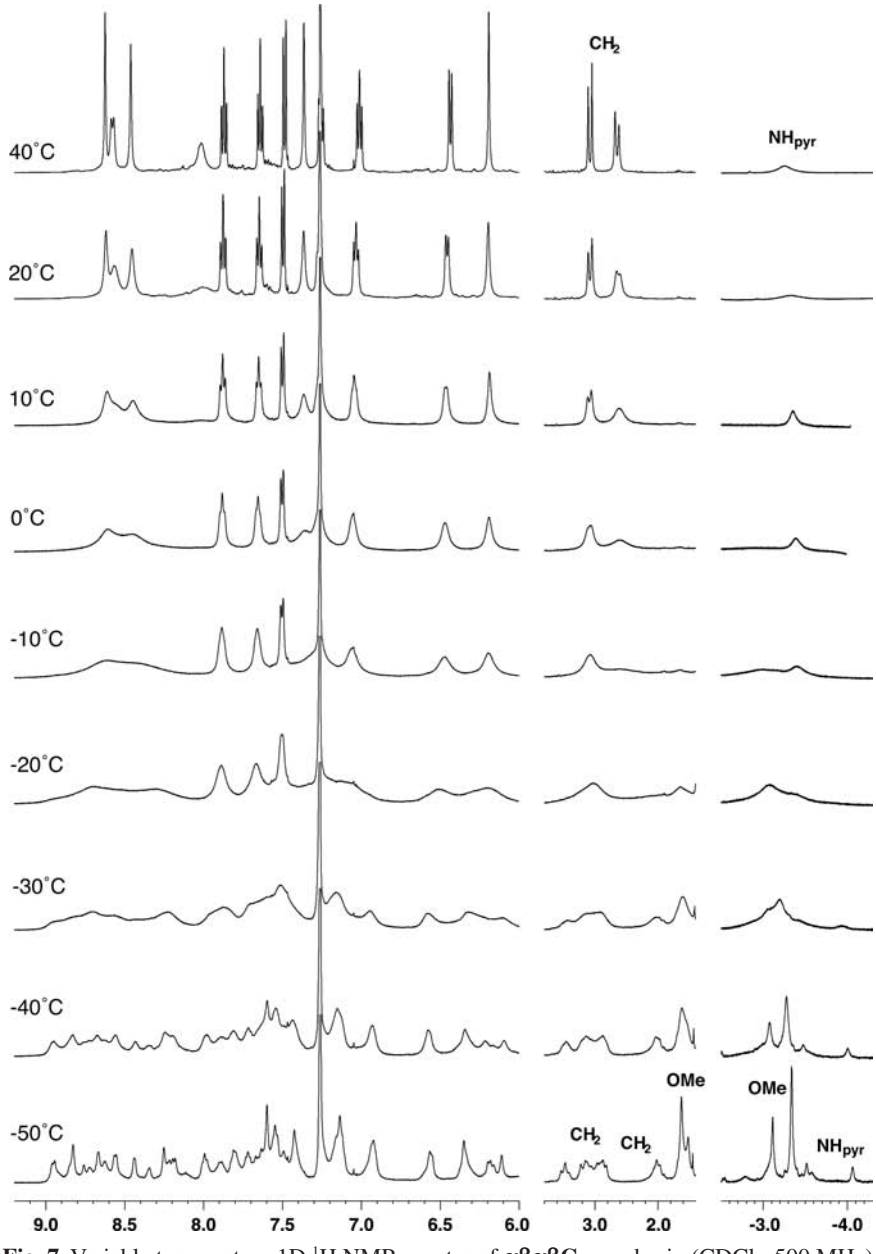

Fig. 7. Variable temperature 1D ^{1}H NMR spectra of $\alpha\beta\alpha\beta\mathbf{C_2}$ porphyrin ($CDCl_3$, 500 MHz).

each other). The unambiguous assignments of aromatic groups were facilitated by comparison with the ^{1}H, ^{13}C assignments obtained at room temperature. In particular, for each resonance, the average of the chemical shifts of the four states should be close to the fast-exchange averaged chemical shift value observed at room temperature. The chemical shift comparison of each resonance in the four states shows that methoxy groups exhibit the largest variation (5.7 ppm) and that the CH resonances at positions 3 and 6 in the phenyl group are also strongly affected. The change in magnetic environment in the phenyl groups could be induced by rotation with respect to the porphyrin ring leading to different orientations. The large change observed in the methoxy groups is probably due to a different positioning with respect to the porphyrin plane associated with two distinct conformations of the binaphthyl handles. Concerted motion of *meso*-phenyl and binaphthyl handles would position alternatively the methoxy group in a proximal or in a distal position with respect to the porphyrin plane, leading to chemical shifts around -3 and +2 ppm, respectively (Fig. 8).

The variable temperature NMR studies performed on $\alpha\beta\alpha\beta\mathbf{C_1}$ porphyrin did not show any exchange phenomenon beside the NH tautomerism of the porphyrin ring [31]. Indeed, the NH- and β-pyrrolic protons exhibit gradual broadening as the temperature is lowered, and signal coalescence occurs around -35 °C (Fig. S1, see Supporting information). Two asymmetric signals are observed for the NH pyrrolic protons at -50 °C, with a ~2:1 intensity ratio. The β-pyrrolic protons that appear as two singlets at room temperature give rise to four signals with two sharp peaks (visible on the HSQC spectrum,

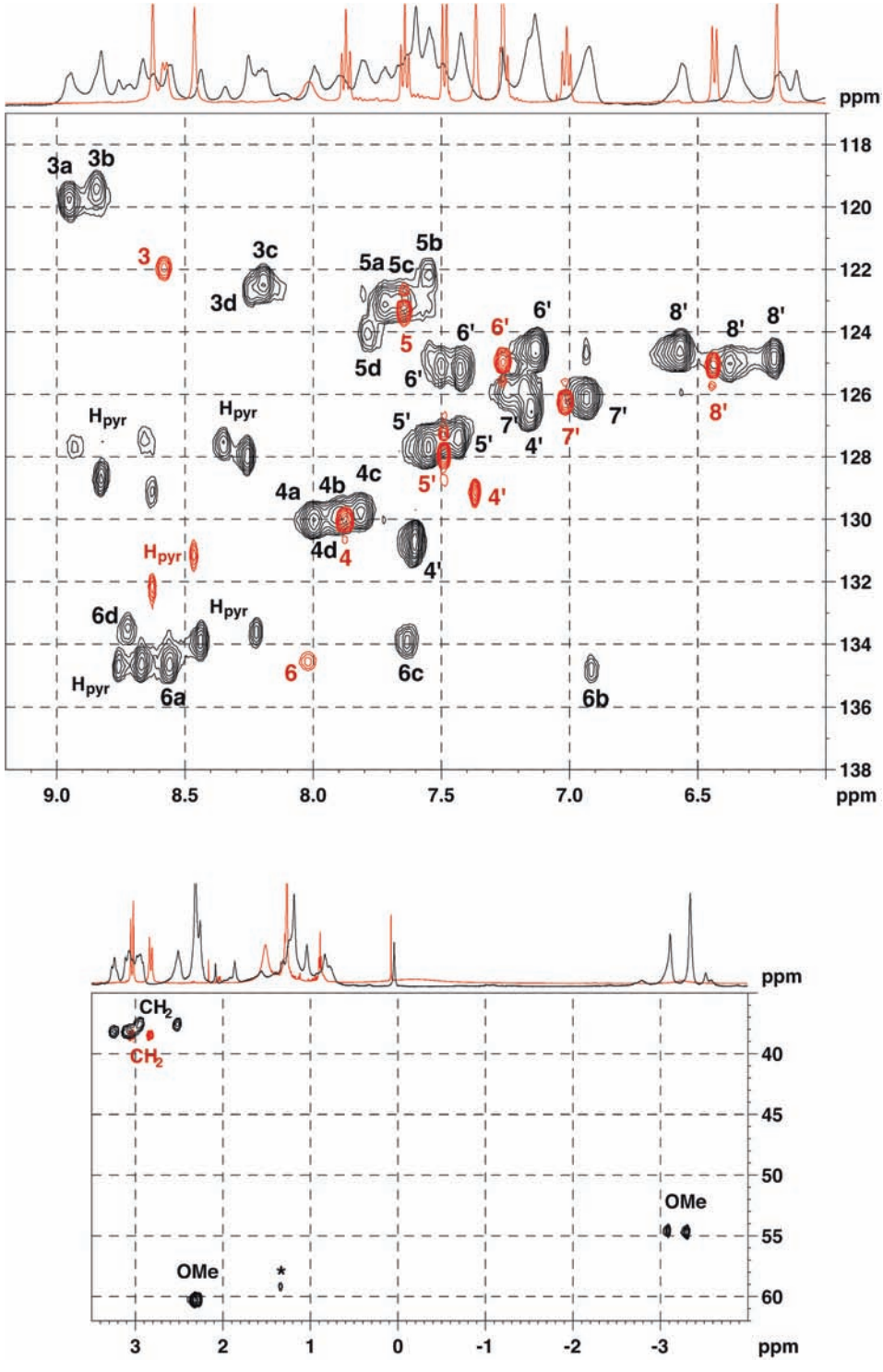

Fig. 8. Superimposition of 2D ^{1}H-^{13}C HSQC spectra of **αβαβC$_2$** porphyrin ($CDCl_3$, 500 MHz) recorded at 40 °C (red) and -50 °C (black). The assignments of the four spin systems of amidophenyl groups are indicated with letters a–d.

Fig. S2) and two broad signals. The signals of pyrrolic protons can be readily interpreted by considering a tautomeric equilibrium in slow exchange on the NMR time scale and because of the chiral environment of the binaphthyl handles. Interestingly, the asymmetric signals observed for the pyrrolic protons indicate that the two tautomeric forms have different stabilities. The methoxy and binaphthyl protons do not show significant changes upon temperature lowering. Protons H_3 and H_6 of the amidophenyl groups exhibit a slight chemical shift variation and the proton H_3 signal becomes significantly more broadened than other signals. These chemical shift variations can be accounted for by their spatial proximity to the porphyrin ring (Fig. S2).

In the case of $\alpha\beta\alpha\beta\mathbf{C_3}$ porphyrin, the NH- and β-pyrrolic protons show similar behavior as in $\alpha\beta\alpha\beta\mathbf{C_1}$ porphyrin upon temperature decreasing (Fig. S3). However, H_3 and H_6 amidophenyl protons and methoxy protons clearly undergo an exchange phenomenon since they show gradual broadening, coalescence and splitting in two signals as the temperature is decreased. For each proton, the two states have close chemical shifts and have different populations, with a ~2:1 intensity ratio. Noteworthy, the protons of both methylene groups also show a variation of their chemical shifts with temperature, and an increase in chemical shift difference is observed between diastereotopic protons at low temperature. Interestingly, the chemical shifts of the methoxy protons in the two states at low temperature strongly differ from the chemical shift at 20 °C, with +0.9 ppm deshielding (Fig. S4).

Catalytic activity toward epoxidation reactions

Epoxidation reactions catalyzed with $\mathbf{Fe\alpha\beta\alpha\beta C_n}$ were examined with iodosylbenzene as the oxidant and excess olefin substrates (catalyst:PhIO:substrate = 1:100:1000) by using the same experimental conditions as the ones previously described for $\mathbf{Fe\alpha\alpha\beta\beta C_n}$ n = 1,2 [3b, 11, 12]. The epoxidation of styrene with the $\mathbf{Fe\alpha\beta\alpha\beta C_1}$ catalyst gave the (*S*)-epoxide as the major product with 38% ee at 25 °C and 54% at -5 °C whereas the ee reached 83% with the $\mathbf{Fe\alpha\alpha\beta\beta C_1}$ catalyst [11, 32]. Furthermore, the activity is lower. Instead of rates of around 40 turnover/min, we observed rates 400 times lower for the epoxidation of styrene. Thus, the active site is hindered by the binaphthyl handle and the olefin approach is difficult, consequently both selectivity and activity diminished. This clearly shows the advantage of an open access to the active site when the same binaphthyl handles $\mathbf{BN_n}$ are attached to the $\alpha\alpha\beta\beta$ geometry. With the homologated catalyst $\mathbf{Fe\alpha\beta\alpha\beta C_2}$, epoxidation of styrene gives the (*R*) epoxide as the major epoxide in 99% yield and 32% ee with a turnover frequency of 15 h^{-1}. Indeed, the active site is more open and the rate is increased by a factor of 2.5. With the $\mathbf{Fe\alpha\beta\alpha\beta C_3}$ catalyst, epoxidation of styrene gives the (*R*) epoxide as the major epoxide in 99% yield and 43% ee with a turnover frequency of 10 h^{-1} and 52% ee at -5 °C. Thus for the $\mathbf{Fe\alpha\beta\alpha\beta C_n}$ porphyrins studied in this work, the results of the epoxidation catalysis show the same particularity as for the $\mathbf{Fe\alpha\alpha\beta\beta C_n}$ porphyrins: the (*S*) epoxide is the major product when the $\mathbf{Fe\alpha\beta\alpha\beta C_1}$ porphyrin is used as catalyst whereas the (*R*) epoxide is the major one when the $\mathbf{Fe\alpha\beta\alpha\beta C_2}$ and $\mathbf{Fe\alpha\beta\alpha\beta C_3}$ catalysts are used.

DISCUSSION

We have shown previously that relevant information on the conformation of binaphthyl handle-free porphyrins $\mathbf{\alpha^2\beta^2 C_n}$ can be obtained from ^{1}H NMR chemical shift analysis. In particular, the methoxy groups which resonate at two different frequencies in $\mathbf{\alpha^2\beta^2 C_n}$ porphyrins play the role of privileged spectators of the environment of the porphyrin. The proximal MeO group which is located near the center of the porphyrin resonates at low frequencies and the distal one which points outward from the tetrapyrrolic core is not affected as much by the anisotropic current of the porphyrin ring and resonates at higher frequency (Table 3, entries 1,4,7). The chemical shifts of the proximal methoxy groups in $\mathbf{\alpha^2\beta^2 C_1}$ and $\mathbf{\alpha^2\beta^2 C_2}$ are negative, which correspond to huge shieldings of 4.09 and 3.78 ppm, respectively (entries 3 and 6). The shielding $\Delta\delta$ is the difference of chemical shift of the methoxy group of 2-methoxy, 3-amido-binaphthyl derivatives $\mathbf{BINAP_n}$ (n = 1–3) (Table 3, entries 2,5,8) that we prepared independently and the chemical shift of the methoxy group of the free porphyrins $\mathbf{\alpha^2\beta^2 C_n}$ (Table 3, entries 1,4,7). These high shieldings had also been encountered for the terephthalic protons C_6H_4 in the handle of the gyroscope porphyrin **3** and basket handle porphyrin **4** (Fig. 6). For example, the shieldings were 4.43 and 4.03 ppm in the same solvent $CDCl_3$ for **3b** and **4** R=Me [33].

For porphyrins $\mathbf{\alpha\beta\alpha\beta C_n}$, the methoxy groups are also spectators of the porphyrin environment. Therefore the observation of exchange-broadened methoxy groups in the case of the C_2 derivative was particularly intriguing and was further investigated to get information on the position of the binaphthyl handles with respect to the porphyrin plane. The comparison of the ^{1}H, ^{13}C NMR chemical shifts for the three $\mathbf{\alpha\beta\alpha\beta C_n}$ porphyrins and their change with temperatures yield interesting information on the different populations adopted by these systems and the dynamics of their conformational equilibria. The short, constrained amide handle in $\mathbf{\alpha\beta\alpha\beta C_1}$ porphyrin leads to significant deviation from planarity of the porphyrin ring, in comparison with $\mathbf{\alpha\beta\alpha\beta C_2}$ and $\mathbf{\alpha\beta\alpha\beta C_3}$ porphyrins. The small temperature dependency of the chemical shift of protons in $\mathbf{\alpha\beta\alpha\beta C_1}$ suggests that the overall structure is quite rigid. The signals of the binaphthyl handle are barely affected by the tautomerism in the porphyrin ring and remain symmetric in the studied temperature range (-50 °C to +40 °C). The deformation of the porphyrin ring should, *a priori*, push away the $\mathbf{\alpha\beta\alpha\beta C_1}$ binaphthyl handle but the reverse cannot be excluded with an approach of the handles towards the deformed porphyrin. Indeed, this kind of deformation had been observed in the case of a Ni-terephthalic, pyridinic bis-handle porphyrin **ArPyNi** for which an X-ray structure showed precisely the deformation of both handles towards the deformed porphyrin plane (Fig. 9). Indeed, the distance between the porphyrin and the distal strap is 3.4 Å, the shortest distance ever reported for this type of structure. The pyridyl ring of the proximal strap is almost parallel to the 4N plane, the dihedral angle between the two planes is 13.6°. The phenyl cap is parallel to the 4N plane and stands precisely in the apical position of the Ni atom at 3.40 Å [34]. The macrocycle exhibits a ruffled conformation [35]: the average Cm deviation is 0.52 Å with respect to

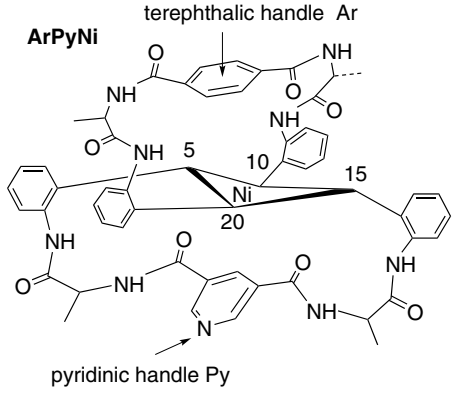

Fig. 9. Schematic representation of the X-ray structure of **ArPyNi**

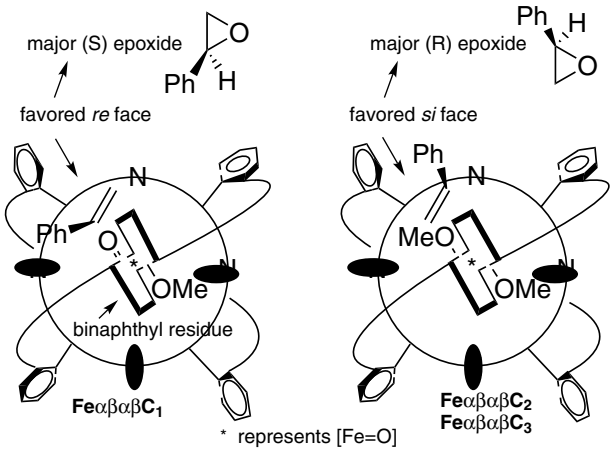

Fig. 10. Possible approach of the olefins toward the Fe=O active site in **FeαβαβC_1** porphyrin

the 24-atom least-squares plane and the average dihedral angle of two opposite pyrrole planes is 32.9°.

The presence of the two methylene linkers in **αβαβC_3** porphyrin removes the steric strain since the porphyrin ring is more planar. This porphyrin is also more flexible, as suggested by the strong temperature dependency of the chemical shifts of methoxy and methylenic protons. Indeed, the chemical shift variations can be interpreted by considering a conformational equilibrium with increased population differences at low temperatures. In the conformer(s) stabilized at low temperature, the methoxy groups are less shielded and would point away from the porphyrin ring. The protons are also sensitive to the tautomerism in the porphyrin ring since two slightly different sets of chemical shifts are observed for protons in the vicinity of the porphyrin under slow exchange conditions.

The **αβαβC_2** porphyrin shows unexpected features, with the presence of up to four states under slow exchange conditions and large chemical shift variations. These four environments can be grouped in two subsets of two states showing close chemical shifts, which splitting could be due to the tautomerism of the porphyrin ring, as observed in **αβαβC_3** porphyrin. In each subset, unequal intensities are observed for the two forms, underlining different stabilities of the two porphyrin systems. The larger chemical shift difference between the two subsets, in particular for methoxy signals, can be explained by a dynamic equilibrium affecting the binaphthyl handles. Thus, the handles interconvert between two conformations with respect to the porphyrin ring. The considerable change in magnetic environments experienced by methoxy groups clearly indicates that they alternatively adopt a *highly shielded proximal position* (–3 ppm) and a *less shielded distal position* with respect to the porphyrin ring (2 ppm). Similar chemical shift values have been observed in **αααββC_2** porphyrins having the same binaphthyl handles but with different attachments to the *meso* 5,10 and 15,20 2-aminophenyl groups, in which methoxy groups have two different environments, inside and outside the porphyrin core. The ^{13}C chemical shift variations at 3 and 4′-positions also suggest orientation changes of amidophenyl and naphthyl groups that are probably concerted with methoxy motions. The interconversion between the two low-energy conformations of the binaphthyl handles occurs at room temperature on fast exchange on the ^{1}H NMR time scale, giving rise to a time-averaged, symmetric spectrum, with the exception of methoxy groups that are in intermediate exchange.

The comparison of catalytic activities clearly shows the importance of the attachment of the binaphthyl handles BINAP$_i$ toward the *meso*-phenyl groups. Indeed, with the catalysts **αααββC_1** and **αααββC_2**, the ee are excellent and the binaphthyl handles discriminate between the *re* and the *si* approach of styrene whereas with the **αβαβ** catalysts, the ee cannot be compared and the handle, too close to the active site, prevents the epoxidation from occurring at a good rate. Thus, this study shows that the active site must be open enough and that the binaphthyl handles attached to the 5,10- and 15,20-*meso*-carbons is the best compromise to afford good yields, enantiomeric excesses and rates. The lengths of the binaphthyl handles in the **αβαβC_n** compounds influence the selectivity of the reaction. We could suggest that the **FeαβαβC_1** complex, as in the **FeαααββC_1** case, is transformed into a quinone type intermediate. The styrene approach with its large phenyl group occupying the space next to the outward leaning lobe, represents the favored low energy path. This leads to the major (*S*)-epoxide *via* a *re* face approach of the olefin towards the [Fe=O] active site. With the **FeαβαβC_2** and **FeαβαβC_3** catalysts, the (*R*) styrene epoxide is recovered as the major one which corresponds to the *si* face approach of the olefin towards the active site in order to avoid the methoxy group (Fig. 10).

EXPERIMENTAL

General information

All reagents were used as supplied commercially unless otherwise noted. THF and diethyl ether were

distilled from sodium under N_2 before use. **BINAP$_n$** [12, 16], αβαβ and ααββ-*o*-TAPP were prepared according to literature method [1]. ^{1}H and ^{13}C NMR spectra were recorded on a Bruker ARX200, a Bruker Avance 400, a Bruker DRX 500 or a Bruker Avance III 500 MHz spectrometer equipped with a TCI cryoprobe. All chemical shifts are in ppm and referenced to solvent signals: 7.26 ppm and 77.16 ppm for ^{1}H and ^{13}C spectra in $CDCl_3$, 7.16 ppm and 128.06 ppm for ^{1}H and ^{13}C spectra in C_6D_6. All the coupling constants are in Hertz (Hz). Infrared spectra were recorded on a Nicolet-Avatar 320 FT-IR. UV-vis spectra were recorded on UVIKON 923 Spectrometer. Wavelengths (λ) are in nanometers (nm). MS/HRMS were obtained at the UPMC. Enantiomeric excess were determined on a Varian CP-3380 gas chromatograph equipped with flame ionization detector and a Cyclodex B 236M capillary column (50 m × 0, 25 μM, DF=0, 25 μM) and using helium as a vector gas.

Synthesis

Synthesis of (R)-(-)-2,2′-dimethoxy-N^3,N$^{3'}$-diphenyl-1,1′-binaphthyl-3,3′-dicarboxamide BINAP$_1$. To a solution of Et_3N (0.158 mL, 1.124 mmol) and freshly distilled aniline (0.1 mL, 1.18 mmol) in 3 mL of dichloromethane was added dropwise a solution of diacid chloride **BN$_1$** (225 mg, 0.559 mmol) in 4 mL of dry dichloromethane. The mixture was stirred overnight at room temperature. The yellow solution was then extracted with water, saturated $NaHCO_3$ solution and HCl 3N. The organic layer was dried over $MgSO_4$ and the solvents evaporated to give a yellow solid that was purified by chromatography column on silica gel (SiO_2 15–40 μm, cyclohexane/dichloromethane: 1/9) to afford the desired product as a yellow thick solid (102 mg, 33%). ^{1}H NMR (400 MHz, $CDCl_3$, 298 K): δ_H, ppm 3.46 (6H, s, O*Me*), 7.16 (2H, m, $H_{5'}$), 7.37–7.42 (2H + 6H, m, $H_{6'}$, H_{Ar}), 7.53 (2H, td, ^3J = 8.2 Hz, ^4J = 1.2 Hz, $H_{7'}$), 7.76 (4H, dd, ^3J = 8.2 Hz, ^4J = 1.2 Hz, H_{Ar}), 8.11 (2H, d, ^3J = 7.9 Hz, $H_{8'}$), 9.01 (2H, s, $H_{4'}$), 9.98 (2H, s, N*H*). ^{13}C NMR (100 MHz, $CDCl_3$, 298 K): δ_C, ppm 62.2 (OMe), 120.3 (C_{Ar}), 124.6 (C_{Ar}), 125.5 ($C_{5'}$), 125.8 (C_q), 126.3 ($C_{7'}$), 127.3 (C_q), 129.0 ($C_{6'}$), 129.2 (C_{Ar}), 129.9 ($C_{8'}$), 130.5 (C_q), 134.7 ($C_{4'}$), 135.5 (C_q), 138.3 (C_q), 153.2 (C_q), 163.2 (CO). HR MS: *m/z* 575.1926 (calcd. for $[C_{36}H_{28}N_2O_4 + Na]^+$ 575.1947). $[\alpha]_D^{20}$: -74.0 (c = 0.5 in THF). Anal. calcd. for $C_{36}H_{28}N_2O_4$: C, 78.24; H, 5.11%. Found: C, 78.31; H, 5.04.

Synthesis of (R)-(+)-2,2′-(2,2′-dimethoxy-1,1′-binaphthyl-3,3′-diyl)bis(N-phenylacetamide) BINAP$_2$. To a solution of Et_3N (80 μL, 0.6 mmol) and freshly distilled aniline (53 μL, 0.562 mmol) in 3 mL of dichloromethane was added dropwise a solution of diacid chloride **BN$_2$** [12] (121 mg, 0.281 mmol) in 4 mL of dry dichloromethane. The mixture was stirred overnight at room temperature. The yellow solution was then extracted with water, saturated $NaHCO_3$ solution and HCl 3N. The organic layer was dried over $MgSO_4$ and the solvents evaporated to give a yellow solid that was purified by chromatography column on silica gel (SiO_2 15–40 μm, cyclohexane/dichloromethane: 1/9) to afford the desired product as a yellow golden solid (129 mg, 79%). ^{1}H NMR (400 MHz, $CDCl_3$, 298 K): δ_H, ppm 3.27 (s, 6H, O*Me*), 3.90 (2H, d, ^2J = 14.4 Hz, $CH_{2\ benz}$), 4.03 (2H, d, ^2J = 14.4 Hz, $CH_{2\ benz}$), 7.02 (2H, td, ^3J = 8.1 Hz, ^4J = 0.9 Hz, H_{Ar}), 7.20–7.28 (2H + 6H, m, $H_{5'}$+H_{Ar}), 7.41–7.46 (6H, m, $H_{7'}$+H_{Ar}), 7.89 (2H, dd, ^3J = 8.1 Hz, ^4J = 1.2 Hz, $H_{8'}$), 8.02 (2H, s, $H_{4'}$), 8.07 (2H, s, N*H*). ^{13}C NMR (100 MHz, $CDCl_3$, 298 K): δ_C, ppm 41.3 ($CH_{2\ benz}$), 61.0 (OMe), 119.7 (C_{Ar}), 124.2 ($C_{6'}$), 125.6 ($C_{5'}$), 125.7 ($C_{7'}$), 124.7 (C_q), 128.1 ($C_{8'}$), 128.5 (C_q), 129.0 (C_{Ar}), 130.9 (C_q), 131.3 ($C_{4'}$), 133.9 (C_q), 138.2 (C_q), 154.5 (C_q), 169.3 (CO). HR MS: *m/z* 603.2238 (calcd. for $[C_{38}H_{32}N_2O_4 + Na]^+$ 603.2260). $[\alpha]_D^{20}$: +6.4 (c = 0.5 in THF). Anal. calcd. for $C_{38}H_{32}N_2O_4$: C, 78.60; H, 5.04. Found: C, 78.49; H, 5.11.

Synthesis of (R)-(-)-3,3′-(2,2′-dimethoxy-1,1′-binaphthyl-3,3′-diyl)bis(*N*-phenylpropanamide) BINAP$_3$. To a solution of Et_3N (70 μL, 0.5 mmol) and freshly distilled aniline (50 μL, 0.497 mmol) in 3 mL of dichloromethane was added dropwise a solution of diacid chloride **BN$_3$** [16] (102 mg, 0.222 mmol) in 4 mL of dry dichloromethane. The mixture was stirred overnight at room temperature. The yellow solution was then extracted with water, saturated $NaHCO_3$ solution and HCl 3N. The organic layer was dried over $MgSO_4$ and the solvents evaporated to give an orange oil that was purified by chromatography column on silica gel (SiO_2 15–40 μm, cyclohexane/dichloromethane: 1/9) to afford the desired product as an orange thick solid (84 mg, 62%). ^{1}H NMR (400 MHz, $CDCl_3$, 298 K): δ_H, ppm 2.87–2.94 (4H, m, $CH_{2\ benz'}$), 3.19 (6H, s, O*Me*), 3.27–3.36 (4H, m, $C_{H2\ benz}$), 7.07 (2H, t, ^3J = 7.6 Hz, H_{Ar}), 7.12 (2H, d, ^3J = 8.1 Hz, ^4J = 0.9 Hz, $H_{5'}$), 7.17 (2H, td, ^3J = 8.1 Hz, ^4J = 1.2 Hz, $H_{6'}$, H_{Ar}), 7.24–7.29 (4H, m, H_{Ar}), 7.36 (2H, td, ^3J = 8.1 Hz, ^4J = 1.2 Hz, $H_{7'}$), 7.55 (d, ^3J = 7.7 Hz, 4H, H_{Ar}), 7.85 (2H, s, $H_{4'}$). 8.42 (2H, s, N*H*). HR MS: *m/z* 631.2551 (calcd. for $[M + Na]^+$ 631.2573). $[\alpha]_D^{20}$: -9.8 (c = 0.5 in THF). Anal. calcd. for $C_{40}H_{36}N_2O_4$: C, 78.92; H, 5.96%. Found: C, 78.76; H, 5.81.

Synthesis of αβαβC$_1$ basket handle porphyrin. A 500 mL two-neck round-bottom flask equipped with a rubber and an argon inlet is charged with 150 mL of freshly distilled tetrahydrofuran on sodium. Freshly dried *N,N*-diethylanilin (0.18 mL, 2.08 mmol) was added. In another flask under argon, αβαβ-tetra-aminophenylporphyrin **TAPPH$_2$** [1] (180 mg, 0.26 mmol) was dissolved in 20 mL of tetrahydrofuran and the resulting solution is transferred into two well-dried 10 mL syringes. The freshly synthesized diacid chloride **BN$_1$** [12] (0.55 mmol) was dissolved in 10 mL of dichloromethane and loaded into a dried 10 mL syringe. A syringe pump was equipped with the three syringes, and the reactants were simultaneously added in the two-neck flask over 2 h at 0 °C. Then the red solution was allowed to stir at room temperature

overnight. The solvent was then removed under vacuum, and the dark purple residue purified by chromatography column on silica gel (SiO_2 15 µm, eluent dichloromethane/methanol: 99/1) to afford the bis-strapped porphyrin as a red-purple solid (318 mg, 87%). ^{1}H NMR (500 MHz, $CDCl_3$, 293 K): δ_H, ppm -2.06 (2H, br s, NH_{pyr}), 0.15 (12H, s, O*Me*), 6.00 (4H, dd, ^3J = 8.6 Hz, ^4J = 0.7 Hz, $H_{8'}$), 6.85 (4H, ddd, ^3J = 8.5 Hz, ^3J = 6.7 Hz, ^4J = 1.2 Hz, $H_{7'}$), 7.12 (4H, ddd, ^3J = 8.3 Hz, ^3J = 6.7 Hz, ^4J = 0.9 Hz, $H_{6'}$), 7.49 (4H, s, N*H*), 7.63 (4H, d, ^3J = 8.2 Hz, $H_{5'}$), 7.68 (4H, td, ^3J = 7.6 Hz, ^4J = 1.2 Hz, H_5), 7.84 (4H, td, ^3J = 8.0 Hz, ^4J = 1.5 Hz, H_4), 8.36 (4H, s, $H_{4'}$), 8.45 (4H, dd, ^3J = 8.3 Hz, ^4J = 1 Hz, H_3), 8.57 (4H, dd, ^3J = 7.5 Hz, ^4J = 1.6 Hz, H_6), 8.66 (4H, s, H_β), 8.80 (4H, s, H_β). ^{13}C NMR (125 MHz, $CDCl_3$, 293K): δ_C, ppm 58.4 (OMe), 113.6 (C_{meso}), 122.8 ($C_{1'}$), 123.7 (C_3), 123.9 (C_5), 124.4 ($C_{8'}$), 124.5 ($C_{3'}$), 125.6 ($C_{6'}$), 128.4 ($C_{7'}$), 129.17 ($C_{5'}$), 129.19 ($C_{4'a}$), 130.0 (C_4), 131.6 (C_β), 131.9 (C_1), 132.4 (C_β), 132.7 (C_6), 134.3 ($C_{4'}$), 135.0 ($C_{8'a}$), 139.5 (C_2), 151.3 ($C_{2'}$), 163.0 (C_{CO}). HR MS: *m/z* 1430.4615 (calcd. for [$C_{92}H_{62}N_8O_8$+Na] 1430.4622). UV-vis (CH_2Cl_2): λ_{max}, nm (log ε) 423 (5.54), 517 (4.40), 550 (3.07), 590 (3.90), 645 (3.40). Anal. calcd. for $C_{92}H_{62}N_8O_8$: C, 78.51; H, 4.44%. Found: C, 78.32; H, 4.29.

Synthesis of αβαβC_2 basket handle porphyrin. A 250 mL two-neck round-bottom flask equipped with a rubber and an argon inlet is charged with 150 mL of freshly distilled tetrahydrofuran on sodium. Freshly dried *N,N*-diethylanilin (0.4 mL, 4.59 mmol) was added. In another flask under argon, αβαβ-tetra-aminophenylporphyrin **TAPPH$_2$** (303 mg, 0.45 mmol) was dissolved in 20 mL of tetrahydrofuran and the resulting solution is transferred into two well dried 10 mL syringes. The freshly synthesized diacid chloride **BN$_2$** [12] (439 mg, 1 mmol) was dissolved in 10 mL of dichloromethane and loaded into a dried 10 mL syringe. A syringe pump was equipped with the three syringes, and the reactants were simultaneously added in the two-neck flask over 3 h at 0 °C. Then the red solution was allowed to stir at room temperature overnight. The solvent was then removed under vacuum, and the dark purple residue purified by chromatography column on silica gel (SiO_2 15 µm, eluent dichloromethane/methanol: 99/1) to afford the bis-strapped porphyrin as a red-purple solid (220 mg, 35%). ^{1}H NMR (500 MHz, $CDCl_3$, 293 K): δ_H, ppm -3.31 (2H, br s, NH_{pyr}), ~0 (12H, vbr s, O*Me*), 2.82 (4H, br d, ^3J = 14 Hz, C$H_{2\ benz}$), 3.04 (4H, d, ^3J = 14 Hz, C$H_{2\ benz}$), 6.18 (4H, s, N*H*), 6.46 (4H, d, ^3J = 8.5 Hz, $H_{8'}$), 7.03 (4H, t, ^3J = 7.7 Hz, $H_{7'}$), 7.28 (4H, $H_{6'}$), 7.37 (4H, s, $H_{4'}$), 7.50 (4H, d, ^3J = 8.0 Hz, $H_{5'}$), 7.65 (4H, t, ^3J = 7.4 Hz, H_5), 7.88 (4H, t, ^3J = 7.9 Hz, H_4), 8.00 (4H, br s, H_6), 8.45 (4H, s, H_β), 8.57 (4H, br s, H_3), 8.61 (4H, s, H_β). ^{13}C NMR (125 MHz, $CDCl_3$, 313K): δ_C, ppm 38.4 (C_{benz}), 113.9 (C_{meso}), 121.9 (C_3), 122.3 ($C_{1'}$), 123.1 (C_5), 124.9 ($C_{6'}$), 125.1 ($C_{8'}$), 126.1 ($C_{7'}$), 126.6 ($C_{3'}$), 127.7 ($C_{5'}$), 129.0 ($C_{4'}$), 129.9 ($C_{4'a}$), 130.0 (C_4), 131.0 (C_1), 132.4 ($C_{8'a}$), 131.1 (C_β), 132.2 (C_β), 134.6 (C_6), 138.8 (C_2), 152.9 ($C_{2'}$), 169.1 (C_{CO}). HR MS: *m/z* 1486.5276 ([M + Na] calcd. for $C_{96}H_{71}N_8O_8Na$ 1486.5248). UV-vis (CH_2Cl_2): λ_{max}, nm (log ε) 420 (5.61), 513 (4.31), 546 (3.77), 588 (3.86), 646 (3.53). Anal. calcd. for $C_{96}H_{70}N_8O_8$: C, 78.78; H, 4.82%. Found: C, 78.62; H, 4.91.

Synthesis of αβαβC_3 basket handle porphyrin. A 500 mL two-neck round-bottom flask equipped with a rubber and an argon inlet is charged with 150 mL of freshly distilled tetrahydrofuran on sodium. Freshly dried *N,N*-diethylanilin (0.28 mL, 3.2 mmol) was added. In another flask under argon, αβαβ-tetra-aminophenylporphyrin **TAPPH$_2$** (220 mg, 0.32 mmol) was dissolved in 20 mL of tetrahydrofuran and the resulting solution is transferred into two well dried 10 mL syringes. The freshly synthesized diacid chloride **BN$_3$** [16] (350 mg, 0.7 mmol) was dissolved in 10 mL of dichloromethane and loaded into a dried 10 mL syringe. A syringe pump was equipped with the three syringes, and the reactants were simultaneously added in the two-neck flask over 2 h at 0 °C. Then the red solution was allowed to stir at room temperature overnight. The solvent was then removed under vacuum, and the dark purple residue purified by chromatography column on silica gel (SiO_2 15 µm, eluent petroleum ether/chloroform: 3/7) to afford the bis-strapped porphyrin as a red-purple solid (126 mg, 26%). ^{1}H NMR (500 MHz, $CDCl_3$, 293 K): δ_H, ppm -2.70 (2H, br s, NH_{pyr}), 1.34 (12H, s, O*Me*), 1.50–1.68 (8H, m, C$H_{2\ homobenz}$), 2.26–2.44 (8H, m, C$H_{2\ benz}$), 6.35 (4H, s, N*H*), 6.58 (4H, d, ^3J = 8.5 Hz, $H_{8'}$), 6.97 (4H, td, ^3J = 7.7 Hz, ^4J = 1.0 Hz, $H_{7'}$), 7.22 (4H, td, ^3J = 7.3 Hz, ^4J = 0.8 Hz, $H_{6'}$), 7.44 (4H, td, ^3J = 7.5 Hz, ^4J = 1.2 Hz, H_5), 7.48 (4H, s, $H_{4'}$), 7.61 (4H, d, ^3J = 8.2 Hz, $H_{5'}$), 7.83 (4H, td, ^3J = 8.0 Hz, ^4J = 1.3 Hz, H_4), 7.95 (4H, dd, ^3J = 7.6 Hz, ^4J = 1.3 Hz, H_6), 8.55 (4H, s, H_β), 8.71 (4H, s, H_β), 8.72 (4H, d, ^3J = 8.0 Hz, H_3). ^{13}C NMR (125 MHz, $CDCl_3$, 293 K): δ, ppm 27.2 (C_{benz}), 38.7 ($C_{homobenz}$), 58.9 (OMe), 114.4 (C_{meso}), 121.0 (C_3), 123.0 (C_5), 124.0 ($C_{1'}$), 124.9 ($C_{6'}$), 125.3 ($C_{8'}$), 125.9 ($C_{7'}$), 127.4 ($C_{5'}$), 129.3 ($C_{4'}$), 130.1 (C_4), 130.4 (C_1, $C_{4'a}$), 131.1 (C_β), 132.1 (C_β), 133.1 ($C_{3'}$, $C_{8'a}$), 134.3 (C_6), 138.8 (C_2), 153.9 ($C_{2'}$), 170.6 (C_{CO}). HR MS: *m/z* 1542.5858 (calcd. for [M + Na] 1542.5874). UV-vis (CH_2Cl_2): λ_{max}, nm (log ε) 419 (5.56), 514 (4.41), 547 (3.88), 587 (3.94), 643 (3.52). Anal. calcd. for $C_{100}H_{78}N_8O_8$: C, 79.03; H, 5.17%. Found: C, 78.96; H, 5.28.

Standard iron metalation procedure. In a typical experiment, **αβαβC_n** free-base (10 mg, 7 µmol) and $FeBr_2$ (50 mg, 0.23 mmol) were added to glacial acetic acid (5 mL) and brought to reflux under argon for 48 h for the **αβαβC_1** porphyrin, 8 h at 90 °C for the **αβαβ**porphyrin and for 4 h at 90 °C for the **αβαβC3** porphyrin. After this reaction time, UV-vis monitoring confirmed that the reaction had reached completion. Excess of acetic acid was then removed under vacuum, and the residue taken in CH_2Cl_2. The organic phases were washed with dilute HCl (1 M), dried over Na_2SO_4, filtered through a pad of silica gel (SiO_2 20–40 µm) and evaporated to dryness to afford chloro-iron complexes **FeαβαβC_1** in 94% yield,

Fe$\alpha\beta\alpha\beta C_2$ in 95% yield and **Fe$\alpha\beta\alpha\beta C_3$** quantitatively as brown powders. **$\alpha\beta\alpha\beta C_1$FeCl.** HR MS: *m/z* 1461.3971 (calcd. for $[M - Cl + H]^+$ 1461.3962). UV-vis (CH_2Cl_2): λ_{max}, nm 419, 509. **$\alpha\beta\alpha\beta C_2$FeCl.** HR MS: *m/z* 1517.4537 (calcd. for $[M - Cl + H]^+$ 1517.4588). UV-vis (CH_2Cl_2): λ_{max}, nm 417, 509. **$\alpha\beta\alpha\beta C_3$FeCl.** HR MS: *m/z* 1573.5177 (calcd. for $[M - Cl + H]^+$ 1573.5214). UV-vis (CH_2Cl_2): λ_{max}, nm 419, 512.

General procedure for asymmetric olefin epoxidation

In a dry Schlenk tube equipped with a stir bar and purged under argon, is introduced a 1.0 mL solution of dried dichloromethane containing 0.50 µmol of catalyst [17], 500 µmol of olefin and 10.0 µL of internal standard (80.0 µmol of 1,2,4-trichlorobenzene). While stirring vigorously, 100 equivalents (50 µmol, 11 mg) of solid iodosylbenzene is added to the reaction. At appropriate intervals, less than 0.1 mL of the solution is removed from the reaction mixture which is loaded on a 60 µm silica pipette column. Elution with diethyl ether removes everything from the column except the catalyst and unreacted iodosylbenzene. The filtrate is then concentrated under nitrogen flux, and a 2 µL sample is shot into the chiral GC column [18] for yield, turnover number and enantiomeric excess analysis. GC retention times for styrene oxides: 24.59 min for the (*R*) epoxide and 25.34 min for the (*S*) epoxide.

Low-temperature experiments

Low-temperature experiments were carried out using the standard epoxidation procedure with one difference that the reaction mixture is cooled in acetone bath, using a cryogenic cooling system, to the desired temperature (-15 °C, -5 °C or 0 °C) before adding the iodosylbenzene [19].

CONCLUSION

We have prepared three chiral binaphthyl porphyrins **$\alpha\beta\alpha\beta C_n$** n = 1–3 in which the binaphthyl handles are attached to the 5,15 and 10,20-*meso*-carbons. The NMR spectra of these porphyrins have been compared to the binaphthyl porphyrins **$\alpha\alpha\beta\beta C_n$** n = 1–3 that we had previously studied. In one case, the **$\alpha\beta\alpha\beta C_2$** porphyrin showed unexpected, intermediate exchange-broadened methoxy groups. Variable temperature NMR studies showed that the methoxy group in **$\alpha\beta\alpha\beta C_2$** porphyrin undergoes intermediate conformational exchange on the ^{1}H NMR time scale at room temperature. Lowering the temperature down to -50 °C revealed the presence of four states in slow exchange on the NMR time scale. These results evidence a dynamic conformational equilibrium of the binaphthyl handles that adopt different, non-symmetric positions with respect to the porphyrin plane. However, the **Fe$\alpha\beta\alpha\beta C_n$** porphyrins, n = 1–3, are not as good catalysts as the corresponding **Fe$\alpha\alpha\beta\beta C_n$** porphyrins for the epoxidation of styrene, the best ee being only 52% for the formation of the (*R*) styrene oxide.

Acknowledgements

We express our thanks to Prof. B. Andrioletti, Drs. E. Brulé, S. Fantauzzi, C. Piangiolino, F. Rose-Munch and students W. Assaf, A. Eloi and M. Poizat for contributing to this work. E. Rose thanks the CNRS for their financial support and E. Rose and E. Gallo thank Galileo program for a HC grant. O. Lequin thanks E. Miclet for fruitful discussion.

Supporting information

Figures S1–S4 are given in the supplementary material. This material is available free of charge *via* the Internet at http://www.worldscinet.com/jpp/jpp.shtml.

REFERENCES

1. Collman JP, Gagne RR, Reed CA, Halbert TR, Lang G and Robinson WT. *J. Am. Chem. Soc.* 1975; **97**: 1427–1439.
2. Collman JP, Ghosh S, Dey A and Decreau RA. *Proc. Natl. Acad. Sci.* 2009; **106**: 22090–22095.
3. a) Collman JP, Zhang X, Lee VJ, Uffelman ES and Brauman JI. *Science* 1993; **261**: 1404–1411. b) Rose E, Andrioletti B, Zrig S and Quelquejeu-Etheve M. *Chem. Soc. Rev.* 2005; **34**: 573–583.
4. a) Lai TS, Chan FY, So PK, Ma DL, Wong KY and Che CM. *Dalton Trans* 2006; 4845–4851. b) Ferrand Y, Le Maux P and Simonneaux G. *Org. Lett.* 2004; **6**: 3211–3214. c) Berkessel A, Kaiser P and Lex J. *Chem. Eur. J.* 2003; **9**: 4746–4756. d) Hamaker CG, Djukic JP, Smith DA and Woo LK. *Organometallics* 2001; **20**: 5189–5199. e) Djukic JP, Young VG Jr and Woo LK. *Organometallics* 1994; **13**: 3995–4003. f) Callot HJ and Piechocki C. *Tetrahedron Lett.* 1980; **21**: 3489–3492. g) Maxwell JL, O'Malley S, Brown KC and Kodadek T. *Organometallics* 1992; **11**: 645–652. h) Simonneaux G and Le Maux P. *Coord. Chem. Rev.* 2002; **228**: 43–60.
5. a) Fantauzzi S, Caselli A and Gallo E. *J. Chem. Soc. Dalton* 2009; **26**: 5434–5443. b) Subbaryan V, Ruppel JV, Zhu S, Perman JA and Zhang XP. *J. Chem. Soc. Chem. Comm.* 2009; 4266–4268.
6. Lu HJ, Subbarayan V, Tao JR and Zhang XP. *Organometallics* 2009; **29**: 389–393.
7. Caselli A, Gallo E, Fantauzzi S, Morriacchi S, Ragaini S and Cenini S. *Eur. J. Inorg. Chem.* 2008; **19**: 3009–3019.
8. a) Naruta Y. In *Metalloporphyrins in Catalytic Oxidations*, Sheldon RA. (Ed.) Dekker M: New York, 1994; pp 241–256. b) Suslick K. In *The Porphyrin Handbook*, Vol. 4, Kadish KM, Smith KM and Guilard R. (Eds.) Academic Press: 2000; pp 41–63 (Chapter 28). c) Marchon JC and Ramasseul R.

In *The Porphyrin Handbook*, Vol. 11, Kadish KM, Smith KM and Guilard R. (Eds.) Academic Press: 2003; pp 75–132 (Chapter 64). d) Boitrel B and Baveux-Chambenoît V. *New J. Chem.* 2003; 942–947.

9. a) Groves JT, Nemo TE and Myers RS. *J. Am. Chem. Soc.* 1979; **101**: 1032–1033. b) Groves JT and Viski P. *J. Org. Chem.* 1990; **55**: 3628–3634. c) Collman JP, Zhang X, Lee VJ and Brauman JI. *J. Chem. Soc. Chem. Comm.* 1992; 1647–1649. d) Groves JT, Crowley SJ and Shalyaev KV. *Chirality* 1998; **10**: 106–119. e) Kossanyi A, Tani F, Nakamura N and Naruta Y. *Chem. Eur. J.* 2001; **7**: 2862–2872. f) Groves JT, Shalyaev K and Lee J. In *The Porphyrin Handbook*, Vol. 4, Kadish KM, Smith KM and Guilard R. (Eds.) Academic Press: 2000; pp 17–39 (Chapter 27).
10. Groves JT and Myers RS. *J. Am. Chem. Soc.* 1983; **105**: 5791–5796.
11. a) Collman JP, Straumanis A, Wang Z, Quelquejeu M and Rose E. *J. Am. Chem. Soc.* 1999; **121**: 460–461. b) Rose E, Quelquejeu M, Pandian RP, Lecas-Nawrocka A, Vilar A, Ricart G, Collman JP, Wang Z and Straumanis A. *Polyhedron* 2000; **19**: 581–586.
12. Rose E, Andrioletti B and Ren QZ. *Chem. Eur. J.* 2004; **10**: 224–230**.**
13. Du G, Andrioletti B, Rose E and Woo LK. *Organometallics* 2002; **21**: 4490–4495.
14. a) Chen Y, Huang L, Ranade MA and Zhang XP. *J. Org. Chem.* 2003; **68**: 3714–3717. b) Penoni A, Wanke R, Tollari S, Gallo E, Musella D, Ragaini F, Demartin F and Cenini S. *Eur. J. Inorg. Chem.* 2003; 1452–1460. c) Huang L, Chen Y, Gao GY and Zhang XP. *J. Org. Chem.* 2003; **68**: 8179–8184.
15. a) Chen Y, Fields KB and Zhang XP *J. Am. Chem. Soc.* 2004; **126**: 14718–14719. b) Chen Y, Gao GY and Zhang XP. *Tetrahedron Lett.* 2005; **46**: 4965–4969. c) Caselli A, Gallo E, Ragaini F, Ricatto F, Abbiati G and Cenini S. *Inorg. Chim. Acta* 2006; **359**: 2924–2932. d) Chen Y and Zhang XP. *Synthesis* 2006; 1697–1700. e) Chen Y and Zhang XP. *J. Org. Chem.* 2007; **72**: 5931–5934. f) Chen Y, Ruppel JV and Zhang XP. *J. Am. Chem. Soc.* 2007; **129**: 12074–12075. g) Zhu S, Ruppel JV, Lu H, Wojtas L and Zhang XP. *J. Am. Chem. Soc.* 2008; **130**: 5042–5043.
16. Fantauzzi S, Gallo E, Rose E, Raoul N, Caselli A, Issa S, Ragaini F and Cenini S. *Organometallics* 2008; **27**: 6143–6151.
17. Depending on the catalyst, since 0.50 μmol typically weighs less than 1 mg, for accurate measurement it is sometimes necessary to weigh out a larger sample of catalyst and make a standard solution.
18. Varian CP-3380 gas chromatograph equipped with flame ionization detector and a Cyclodex B 236M capillary column (50 m × 0.25 μM, DF = 0.25 μM).
19. GC factors: GC factors were calculated to correct the fact that different compounds have different FID sensitivities. In the case of styrene, calibrations curves were constructed with respect to the standard 1,2,4-trichlorobenzene (tcb) so exact yields and turnover numbers are available for epoxidation of this olefin. Factor = (μmol compound/μmol tcb) × (peak area tcb/peak area compound). Styrene oxide (sox): Fsox = 3.25 and iodobenzene (PhI): FPhI = 2.91. Calculation of μmol of styrene oxide (sox) or iodosobenzene (PhI) is as follows: μmolA = μmol tcb × (peak area A/peak area tcb) × FA (A = sox or PhI). GC retention time: 24.59 min for the (*R*) styrene oxide and 25.34 min for the (*S*) styrene oxide.
20. Rose E, Quelquejeu M, Pochet C, Kossanyi A, Julien N and Hamon L. *J. Org. Chem.* 1993; **58**: 5030–5031.
21. Rose E, Cardon-Pilotaz A, Quelquejeu M, Bernard N, Kossanyi A and Desmazières B. *J. Org. Chem.* 1995; **60**: 3919–3920.
22. Zrig S, Andrioletti B and Rose E. *Tetrahedron Lett.* 2005; **46**: 1103–1105.
23. a) Simonis U, Walker FA, Lee PL, Hanquet BJ, Meyerhoff DJ and Scheidt RW. *J. Am. Chem. Soc.* 1987; **109**: 2659–2668. b) Medforth CJ, Berber MD and Smith KM. *Tetrahedron Lett.* 1990; **31**: 3719–3723. c) Wagner RW, Johnson TE and Lindsey JS. *Tetrahedron* 1997; **53**: 6755–6790.
24. a) Renaud P, Battioni P and Mansuy D. *New J. Chem.* 1987; **11**: 279–290. b) Momenteau M, Loock B, Tetreau C, Lavalette D, Croisy A, Schaeffer C, Huel C and Lhoste JM. *J. Chem. Soc. Perkin Trans II,* 1987; 249–257. c) Walkers FA, Buchler J, West JT and Hinds J. L. *J. Am. Chem. Soc.* 1983; **105**: 6923–6929. d) Momenteau M, Locock B, Huel C and Lhoste JM. *J. Chem. Soc. Perkin Trans 1*. 1988; 283–295.
25. Perlmutter P, Rose M and Shenan P. *Tetrahedron Lett.* 1988; **29**: 1427–1430.
26. Boitrel B, Camireilli E, Fleche Y, Lecas A and Rose E. *Tetrahedron Lett.* 1989; **30**: 2923–2926.
27. a) Boitrel B, Lecas A, Renko Z and Rose E. *J. Chem. Soc. Chem. Commun.* 1985; 1820–1821. b) Lecas A, Levisalles J, Renko D and Rose E. *Tetrahedron Lett.* 1984; **25**: 1563–1566. c) Lecas A, Levisalles J, Mariacher C, Renko D and Rose E. *Canad. J. Chem.* 1984; **62**: 2054–2058. d) Lecas A, Renko D and Rose E. *Tetrahedron Lett.* 1985; **26**: 1019–1012. e) Rose E, Andrioletti B and Pandian RP. *J. Porphyrins Phthalocyanines* 2002; **6**: 602–606.
28. a) Boitrel B, Lecas A and Rose E. *Tetrahedron Lett.* 1988; **29**: 5653–5656. b) Boitrel B, Lecas A, Renko Z and Rose E. *New J. Chem.* 1989; **13**: 73–99. c) Boitrel B, Lecas A and Rose E. *Tetrahedron Lett.* 1991; **32**: 2129–2132. d) Boitrel B, Lecas-Nawrocka A and Rose E. *Tetrahedron Lett.* 1992; **33**: 227–230.

e) Rose E, Soleilhavoup M, Christ-Tommasino L, Moreau G, Collman JP, Quelquejeu M and Straumanis A. *J. Org. Chem.* 1998; **63**: 2042–2044. f) Rose E, Quelquejeu M, Kossanyi A and Boitrel B. *Coord. Chem. Rev.* 1998; **178–180**: 1407–1431.

29. a) Rose E, Kossanyi A, Quelquejeu M, Bernard N, Soleilhavoup M, Duwavran F and Lecas A. *J. Am. Chem. Soc.* 1996; **118**: 1567–1568. b) Rose E, Quelquejeu-Etheve M and Andrioletti B. *J. Porphyrins Phthalocyanines* 2003; **7**: 375–381.
30. The first observation is the similar chemical shifts for the **αβαβC2** and **αβαβC3** porphyrin protons (Table 1). However for the **αβαβC1** porphyrin, the chemical shifts of the H4′ and H8′ deserve comments. Indeed, the H4′ protons resonate at a downfield chemical shift of 8.36 ppm and are deshielded by 1.00 ppm with respect to the corresponding protons in **αβαβC2** and **αβαβC3**. This can be explained by an anisotropy effect of the amido group directly linked to the naphthyl residue whereas in the other cases the naphthyl moiety is linked to a methylene group. For the signal of the H8′ proton at 6.00 ppm, the effect of the anisotropy of the macrocycle shields it by a value of 2.11 ppm. The shieldings Δδ for the two other porphyrins are 1.43 ppm for **αβαβC2** and 1.22 ppm for **αβαβC3**.
31. Storm CB and Teklu Y. *J. Am. Chem. Soc.* 1972; **94**: 1745–1747.
32. Epoxidation of limonene was also tested but the ee again are too low to be exploited: 16% ee of the 1,2-limonene epoxide and 32% for the 8,9-limonene epoxide, the ratio of the two epoxides 1.2/8.9 is 2.8/1.
33. Boitrel B, Lecas A and Rose E. *J. Chem. Soc. Chem. Comm.* 1989; 349–350.
34. Richard P, Rose E and Boitrel B. *Inorg. Chem*. 1998; **37**: 6532–6534.
35. a) Sparks LD, Medforth CJ, Park MS, Chamberlain JR, Ondrias MR, Senge MO, Smith KM and Shelnutt JA. *J. Am. Chem. Soc.* 1993; **115**: 581–592. b) Schappacher M, Fischer J and Weiss R. *Inorg. Chem.* 1989; **28**: 389–390.